NON-CRIMP FABRICS GEOMETRICAL VARIABILITY AND ITS INFLUENCE ON COMPOSITES CURE

T.S. Mesogitis[a*], A.A. Skordos[a], A.C. Long[b]

[a]*Composites Centre, Manufacturing and Materials Department, School of Applied Sciences, Cranfield University, Bedford, MK43 0AL, UK*
[b]*Division of Materials, Mechanics & Structures, University of Nottingham, University Park, Nottingham NG7 2RD, UK*
**t.mesogitis@cranfield.ac.uk*

Keywords: variability, non-crimp fabrics, modelling of random field

Abstract

A framework is developed and implemented to characterize and model in plane fibre misalignment in Non-Crimp fabrics (NCF). Image analysis based on fast Fourier Transform and correlation analysis is used to characterise in plane fibre misalignment in a carbon fibre ±45º NCF. It is found that fibre misalignment is significant showing high anisotropic spatial autocorrelation with the major direction of autocorrelation coinciding with the direction of the non-structural stitching of the fabric. The spatial autocorrelation structure of the fabric is modelled using an autoregressive two-dimensional stochastic process, the Ornstein-Uhlenbeck (OU) sheet. The resulting stochastic field is simulated using the Cholesky factorization, the spectral decomposition and the Karhunen-Loeve expansion (KLE). The three discretization techniques are compared in terms of accuracy and efficiency.

1. Introduction

Fibre misalignment is one of the main sources of variability in composite manufacturing. Variability in as supplied dry fabrics and pre-pregs is mainly associated with in plane and out of plane tow waviness setting the minimum level of uncertainty in all subsequent steps of composite manufacturing [1-3]. Fibre misalignment can substantially influence the forming/draping step [2,4] introducing significant uncertainty in the minimum and average wrinkling strain of the formed part [2]. During the forming/draping step the fabric is subjected to considerable shear deformation which may intensify the already existing geometrical heterogeneities. These phenomena can in turn influence the local fibre volume fraction and porosity distribution introducing significant variability in permeability. Several experimental and numerical studies have outlined the effect of fibre angle and fibre spacing variability on permeability variation [5-8]. Fibre misalignment along with fibre volume fraction variations can introduce significant scatter to the mechanical, thermo-mechanical and thermal properties of the constituent materials affecting the curing process [9-10]. This can also introduce uncertainty to the level of residual stresses [11-12]. However, unlike permeability the effect of fibre misalignment on the cure process has not been explicitly investigated with the results being based on conceptual scenario rather than experimental data. Furthermore, fibre architecture plays a crucial role in the structural performance of composite materials governing non-linear phenomena such as failure and damage initiation. It has been shown that

geometrical heterogeneity can significantly affect the compressive strength of the manufactured part [13]. Therefore, a characterisation and modelling approach that would take these effects into consideration explicitly is of crucial importance to allow quantification of process outcome variability within a stochastic simulation framework.

This study aims at the development of a methodology to characterise and model in plane fibre misalignment in NCF. An image analysis methodology is developed and employed to measure local fibre angle variability. A two-dimensional autoregressive stochastic process, the Ornstein-Uhlenbeck (OU) sheet is used to describe the autocorrelation structure of the fabric. Estimation of the autocorrelation parameters is carried out using least squares. The resulting stochastic field is simulated using the Cholesky factorization, the spectral decomposition and the Karhunen-Loeve expansion (KLE). The three discretization techniques are compared in terms of accuracy and efficiency.

2. Image analysis

An in-house image analysis code described in detail in [2] developed to characterise fibre misalignment in woven textiles has been enhanced in order to characterise fibre misalignment in unidirectional materials such as non-crimp fabrics (NCF). The image analysis code is based on Fast Fourier transform and correlation analysis. The approach adopted involves calculation of local fibre direction relative to the fibre orientation of a reference image, so that the spatial random field is explicitly quantified. Fast Fourier transform is employed to obtain a prior estimation of the fibre orientation. The correlation analysis is used for accurate calculation of local fibre orientation using a reference region $r_\theta(x,y)$, which is carried out by rotating a kernel $k_\theta(x,y)$ of size $M \times M$ obtained from a reference image. The reference region is:

$$r_\theta(x,y) = k_\theta(x\cos\theta + y\sin\theta, -x\sin\theta + y\cos\theta) \tag{1}$$

The correlation of a reference region $r_\theta(x,y)$ of size $M \times M$ with the image $f(x,y)$ of size $K \times K$ is calculated as follows [2]:

$$\rho(\theta) = \frac{\sum_{i=1,j=1}^{M,M}\left(r_\theta(x_i,y_i)-\overline{r_\theta}\right)\left(f(x_i,y_j)-\overline{f}\right)}{\sqrt{\sum_{i=1,j=1}^{M,M}\left(r_\theta(x_i,y_j)-\overline{r_\theta}\right)^2\sum_{i=1,j=1}^{M,M}\left(f(x_i,y_j)-\overline{f}\right)^2}} \tag{2}$$

where $\overline{r}_\theta$ and $\overline{f}$ are the average of the $r_\theta(x,y)$ *and* $f(x,y)$ arrays, respectively.

The image analysis procedure is as follows:

- Image acquisition into a discrete pixel array $f(x,y)$.
- Determination of a reference image.
- Application of Fast Fourier transform.
- Calculation of radial energy $E(\theta)$ in polar coordinates.
- Estimation of approximate fibre orientation that maximizes $E(\theta)$.
- Calculation of difference between fibre orientation of reference and current image.
- Calculation of correlation of the current image with the reference image by rotating the reference image using directional cosines.
- Estimation of the angle that maximises correlation.

This methodology was implemented to images of a 6k carbon fibre ± 45º NCF HTS (Hexcel) with a chain knit stitch pattern. The areal density of this fabric is 534 g/m^2. A Sony camera was used to acquire digital images. The camera was mounted on a robotic head in order to control and record the exact position of each image, as shown in Figure 1a. Seven hundred and forty-eight images were acquired from each side (upper/lower) of the ± 45º NCF on a 34×22 grid with 5 mm spacing. The size of the pixel array is 640×480. Application of the fast Fourier transform was carried out on a 256×256 region. Implementation of Eq. (2) is computationally intensive; therefore the size of the reference region was 60×60. The image analysis results are illustrated as two lines; (i) stich orientation, set always at 0º, (ii) calculated tow orientation (Figure 1b). The analysis of statistical properties was carried on the full dataset on a 5 x 5 mm grid and additional datasets on a coarser (10 x 10 mm) and finer (2.5 x 2.5 mm) grid produced using the original images. These additional datasets were utilised to demonstrate that the analysis results in terms of variance and autocorrelation structure do not depend on the grid size. In addition, a series of 50 images were acquired at the same location and analysed to estimate the variance associated with the image acquisition and analysis methodology.

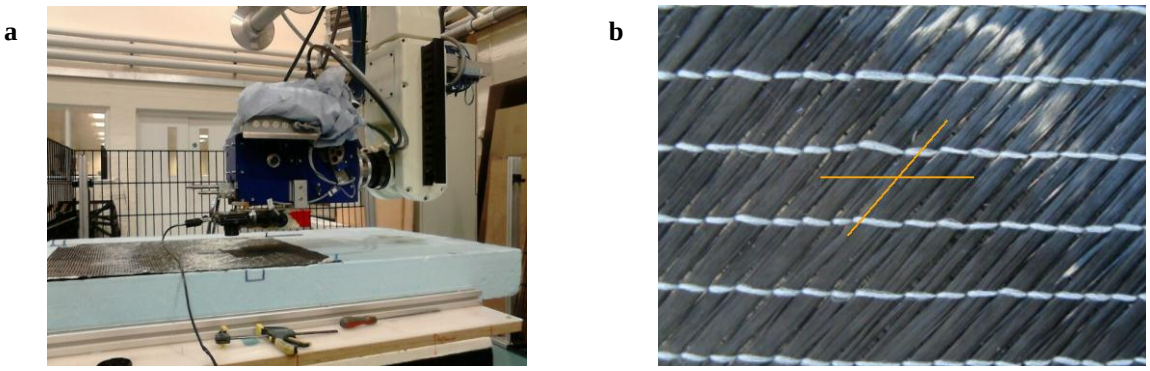

Figure 1. Image analysis of NCF: (a) experimental set-up; (b) image and calculated fibre orientation

3. Statistical properties

The experimental results indicated that both sides present identical statistical behavior in terms of standard deviation and autocorrelation structure. Table 1 summarizes the basic statistical properties of tow orientation of the 6k carbon fibre ± 45º NCF HTS. The probability distributions of the upper and lower side of the ± 45º NCF are depicted in Figure 2a and Figure 2b, respectively. Fibre angles are measured in an anti-clockwise direction relative to the stitch of the fabric (0º) as depicted in Figure 1b. The statistical properties presented in Table 1, include the average μ and the standard deviation σ of the sample field. The fabric shows considerable variability in tow orientation of about 1.2º. This result should be compared with the standard deviation obtained for the set of images from a single location which is 0.1º. The results reported in Table 2 show that there is no correlation between tow orientation of the two sides, implying that variability in tow orientation of the two sides of the fabric is produced independently. Examination of Figure 2 suggests that tow orientation in both sides are normally distributed.

variable	upper side	lower side
μ [º]	45	-45
σ[º]	1.22	1.22

Table 1. Statistical properties of tow orientation of carbon fibre ± 45º NCF

	upper side	lower side
upper side	1	0.014
lower side	0.014	1

Table 2. Correlation matrix of tow orientation of carbon fibre ± 45º NCF

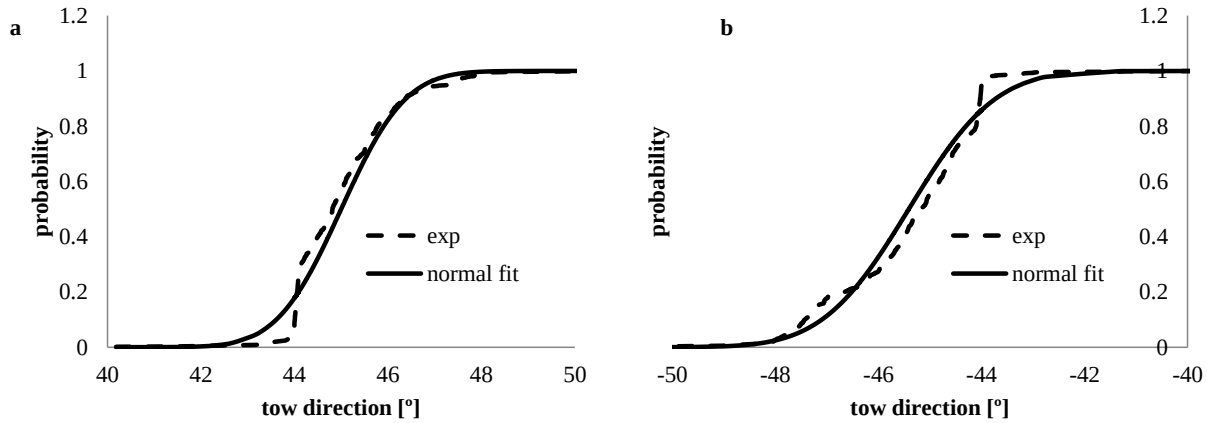

Figure 2. Probability distributions of fibre orientation of carbon fibre ± 45º NCF: (a) upper side; (b) lower side

The autocorrelation structure of the orientation of the tows was investigated in order to estimate the spatial dependence of variability. The method of moments was used to quantify spatial autocorrelation as a function of distance and direction. The correlation between two samples of all pairs of points obtained from the experimental results located at a specific distance and direction was calculated and reported in Figure 3. It can be observed that fibre misalignment of the ± 45º NCF exhibits high anisotropic spatial autocorrelation with the major direction of autocorrelation coinciding with the direction of the stich (0º). Autocorrelation at ±25º directions reaches a value close to zero at about 40 mm, while autocorrelation at ±50º and ±75º directions shows a faster decay reaching zero at approximately 25 mm. It can be observed, that the autocorrelation in opposite directions is very similar, suggesting that the autocorrelation structure of this fabric is quadrant symmetric. Spatial cross-correlation between orientation of the tows of the two sides was found to be negligible.

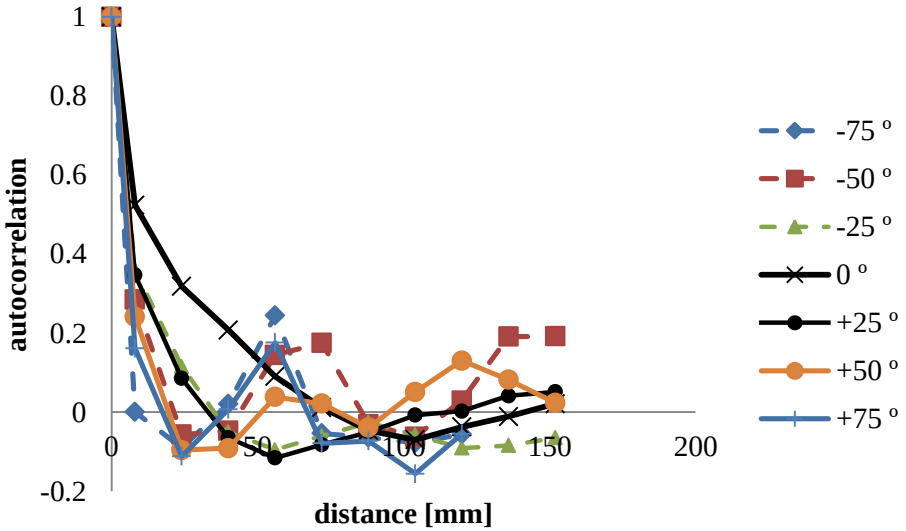

Figure 3. Directional autocorrelation of fibre orientation of carbon fibre ± 45º NCF

4. Stochastic model

4.1 Modelling of the random field

The random field is modelled using a two-dimensional autoregressive stochastic process, the Ornstein-Uhlenbeck sheet (OU), which is a second order stationary Gaussian process with the following auto-covariance function [15,16]:

$$C(x,y)=\sigma^2 e^{-|x_1-x_2|/b_x-|y_1-y_2|/b_y} \tag{3}$$

Here σ is the standard deviation, and b_x, b_y are the correlation lengths, since they determine the decay rate of the autocorrelation structure between two points of the process. Estimation of b_x, b_y was carried out using least squares and it was performed by the Microsoft Excel solver. This approach yielded a value of 20.21 mm for b_x, and 4.67 mm for b_y.

4.1.1 Discretisation of the random field

4.1.1.1 Cholesky factorisation

The Cholesky method decomposes the covariance matrix, Σ as follows:

$$\Sigma = LL^T \tag{4}$$

where *L* is a lower triangular matrix. The product of *L* with the vector *Y* of independent identically distributed normal variables is a vector *V* that encompasses the statistical properties of the random field, and is defined as follows:

$$V = LY \tag{5}$$

4.1.1.2 Spectral decomposition

The spectral decomposition expands the random field *V(x,y)* as a sum of trigonometric functions with random phase angles as a function of its spectral density function $S(k_x,k_y)$ [16]:

$$V(x,y)=\sqrt{2}\sum_{n_x=0}^{N_x-1}\sum_{n_y=0}^{N_y-1}\left[A_{n_xn_y}\cos\left(k_{xn_x}x+k_{yn_y}y+\varphi^{(1)}_{n_xn_y}\right)+\tilde{A}_{n_xn_y}\cos\left(k_{xn_x}x-k_{yn_y}y+\varphi^{(2)}_{n_xn_y}\right)\right] \tag{6}$$

where:

$$A_{n_xn_y}=\sqrt{S(k_{xn_x},k_{yn_y})\Delta k_x\Delta k_y} \quad ; \quad \tilde{A}_{n_xn_y}=\sqrt{S(k_{xn_x},-k_{yn_y})\Delta k_x\Delta k_y} \tag{7}$$

$$k_{in_i}=n_i\Delta k_i \quad ; \quad \Delta k_i=\frac{k_{iu}}{N_i} \quad \text{for } i=x,y \tag{8}$$

k_{xu} and k_{yu} denote the upper cut-off wave numbers, whereas $\varphi^{(1)}_{n_x n_y}$ and $\varphi^{(2)}_{n_x n_y}$ are different sets of random phase angles distributed uniformly over the interval [0,2π]. In the case of the Ornstein-Uhlenbeck sheet, described in Eq. (3), the spectral density function is [17]:

$$S(k_x, k_y) = \frac{\sigma^2}{\pi^2} \frac{b_x b_y}{(1 + b_x^2 k_x^2)(1 + b_y^2 k_y^2)} \tag{9}$$

4.1.1.3 Kahrunen-Loeve expansion

A stationary random field *V(x,y)* can be represented as follows [18]:

$$V(x, y) = \mu + \sum_{i=1}^{M} \sqrt{\lambda_i}\, \varphi_i(x, y) \xi_i \tag{10}$$

where λ_i and $\varphi_i(x, y)$ are the eigenvalues and the eigenfunctions of the covariance function, whereas ξ_i is a set of independent identically distributed normal variables. Given a stochastic process defined over the interval [-*α*,*α*] and [-*β*,*β*] over the x and y direction, with a covariance function as defined by Eq.(3), the eigenvalues and the eigenfunctions are [18]:

for *i* = odd

$$\lambda_i = \sigma^2 \left(\frac{2b_x}{\omega_{xi}^2 + b_x^2} \frac{2b_y}{\omega_{yi}^2 + b_y^2} \right) \quad ; \quad \varphi_i(x, y) = \frac{\cos(\omega_{xi} x)}{\sqrt{\alpha + \dfrac{\sin(2\omega_{xi} a)}{2\omega_{xi}}}} \frac{\cos(\omega_{yi} y)}{\sqrt{\beta + \dfrac{\sin(2\omega_{yi} \beta)}{2\omega_{yi}}}} \tag{11}$$

for *i* = even

$$\lambda_i^* = \sigma^2 \left(\frac{2b_x}{\omega_{xi}^{*2} + b_x^2} \frac{2b_y}{\omega_{yi}^{*2} + b_y^2} \right) \quad ; \quad \varphi_i^*(x, y) = \frac{\sin(\omega_{xi}^* x)}{\sqrt{\alpha - \dfrac{\sin(2\omega_{xi}^* a)}{2\omega_{xi}^*}}} \frac{\sin(\omega_{yi}^* y)}{\sqrt{\beta - \dfrac{\sin(2\omega_{yi}^* \beta)}{2\omega_{yi}^*}}} \tag{12}$$

$$b_j - \omega_{ij} \tan(\omega_{ij} \alpha) = 0 \quad ; \quad \omega_{ij}^{\ *} + b_j \tan(\omega_{ij}^{\ *} \beta) = 0 \quad \text{for } j = x, y \tag{13}$$

4.2 Stochastic simulation

The three discretisation techniques presented were implemented to simulate fibre misalignment of the 6k carbon fibre ± 45º NCF HTS. Figure 3 illustrates the autocorrelation of the simulated tow orientation generated on a 68×22 grid with 5mm spacing. The autocorrelation of the sample field generated using the KLE is not presented due to the poor quality of results. This is attributed to the fact that the performance of the KLE is high only in the case of highly correlated stochastic fields [19]. N_x and N_y (see section 4.1.1.2) were set at 68 and 22, respectively, in order to compare the Cholesky factorisation and the spectral decomposition in terms of accuracy and efficiency. It can be observed that both discretisation techniques can reproduce the stochastic field with very good accuracy, with the discrepancies between the two methods being negligible. Therefore, given the same computational effort, both techniques are deemed capable of modeling fibre misalignment of the fabric of this study, with quite good accuracy.

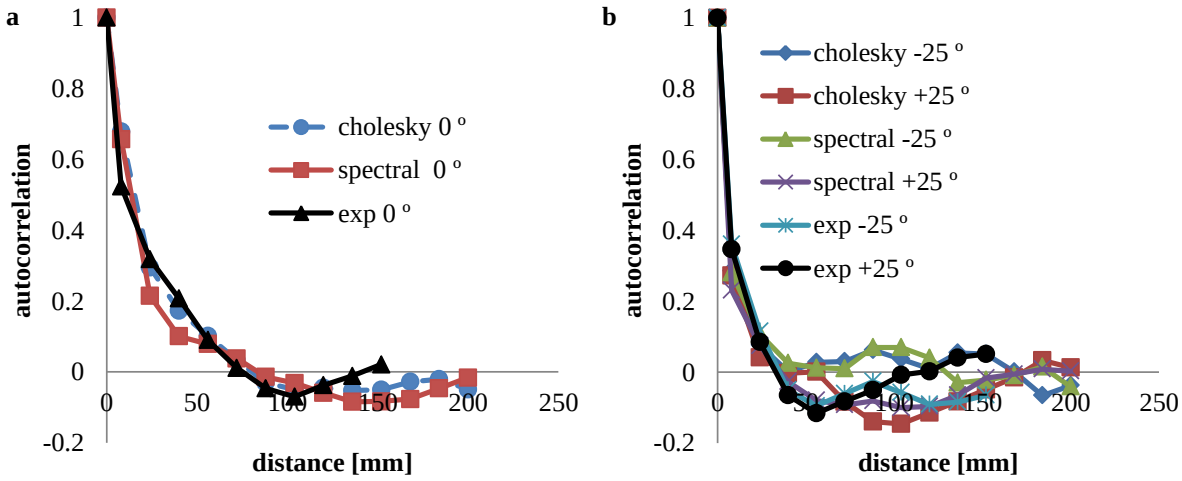

Figure 4. Directional autocorrelation of simulated tow orientation of carbon fibre ± 45º NCF: (a) 0 º, (b) ±25 º

5. Conclusions

A methodology is presented for characterising and modeling fibre misalignment in unidirectional fabrics. Application of image analysis provides quantitative information on misalignment of tows. The analysis is implemented to images of a 6k carbon fibre ± 45º NCF HTS (Hexcel). Fibre misalignment is considerable showing high anisotropic autocorrelation with the major direction of autocorrelation coinciding with the direction of the non-structural stitching of the fabric. It is found that the Cholesky factorisation and spectral decomposition are capable of representing the spatial field accurately with the same accuracy and efficiency. On the contrary, the Kahrunen-Loeve expansion yielded poor results for the given study. The Cholesky method is deemed to be the most appropriate technique to reproduce the stochastic field of this study due to its simplicity in comparison to the spectral decomposition.

The stochastic model of fibre variability can be coupled with a finite element based cure simulation model to quantify the way variability in fibre architecture and the associated variations in the local tensor of in plane thermal conductivity and fibre volume fraction propagate through the curing stage of composites processing. The coupling can be achieved by the incorporation of local fibre direction and areal density information in the material models computing the thermal conductivity tensor, the specific heat capacity and the heat emitted during the curing reaction. The uncertainty in process outcome from fibre misalignment can be compared to that due to other sources of variability such as cure kinetics uncertainty and thermal boundary conditions to evaluate their relative contribution to product reproducibility. The outcome of this work will allow incorporation of variability in process design/optimisation to address robustness – performance trade-offs.

Acknowledgements

This work was supported by the Engineering and Physical Sciences Research Council [grant number: EP/IO33513/1], through the EPSRC Centre for Innovative Manufacturing in Composites (CIMComp).

References

[1] Potter K, Understanding the origin of defects and variability in composites manufacture. In: Proceedings of the 17th International Conference on Composite Materials, Edinburgh, UK, 2009.
[2] Skordos AA, Sutcliffe MPF. Stochastic simulation of woven composites forming. Composites Sci Technol 2008;68(1):283-296.
[3] Verleye B, Lomov SV, Long A, Verpoest I, Roose D. Permeability prediction for the meso–macro coupling in the simulation of the impregnation stage of Resin Transfer Moulding. Composites Part A: Applied Science and Manufacturing 2010;41(1):29-35.
[4] Long A, Wiggers J, Harrison P. Modelling the effects of blank-holder pressure and material variability on forming of textile preforms. In: Proceedings of the 8th international ESAFORM conference on materials forming, Cluj-Napoca, Romania; 2004.
[5]Pan R, Liang Z, Zhang C, Wang B. Statistical characterization of fiber permeability for composite manufacturing. Polym Compos 2000;21(6):996–1006.
[6] Endruweit A, McGregor P, Long AC, Johnson MS. Influence of the fabric architecture on the variations in experimentally determined in-plane permeability values. Compos Sci Technol 2006;66(11–12):1778–92.
[7] Endruweit A, Long AC. Influence of stochastic variations in the fibre spacing on the permeability of bi-directional textile fabrics. Composites Part A 2006;37(5):679–94.
[8] Endruweit A, Long AC, Robitaille F, Rudd CD. Influence of stochastic fibre angle variations on the permeability of bi-directional textile fabrics. Composites Part A 2006;37(1):122–32.
[9] Liaw D, Singhal S, Murthy P, Chamis CC. Quantification of uncertainties in composites. In: Proceedings of the 34th AIAA/ASME/ASCE/AHS/ASC structures, structural dynamics and materials conference, La Jolla, CA, USA; 1993, p. 1163–73.
[10] Chamis CC. Probabilistic composite mechanics assurance for better-cheaperfaster products. In: Proceedings of the 39th AIAA/ASME/ASCE/AHS/ASC structures, structural dynamics, and materials conference and exhibit, Long Beach, CA, USA; 1998. p. 1940–51.
[11] Dong C. Model development for the formation of resin-rich zones in composites processing. Composites Part A 2011;42(4):419–24.
[12] Hubert P, Pipes RB, Grimsley BW. Variability analysis in vacuum assisted resin transfer molding. In: Proceedings of the 23rd SAMPE Europe international conference, Port de Versailles, France; 2002.
[13] Liu D, Fleck NA, Sutcliffe MPF. Compressive strength of fibre composites with random fibre waviness. J Mech Phys Solids 2004;52(7):1481–505.
[14] Terdik G, Woyczynski WA. Notes on fractional Ornstein–Uhlenbeck random sheets. Publ Math Debrecen 2005;66(1–2):53–181.
[15] Arato´ M, Pap G, Van Zuijlen MCA. Asymptotic inference for spatial autoregression and orthogonality of Ornstein–Uhlenbeck sheets. Comput Math Appl 2001;42(1–2):219–29.
[16] Shinozuka M, Deodatis G. Simulation of multi-dimensional Gaussian stochastic fields by spectral representation. Appl Mech Rev 1996;49:29-53.
[17] Stefanou G, Papadrakakis M. Assessment of spectral representation and Karhunen–Loève expansion methods for the simulation of Gaussian stochastic fields. Comput Methods Appl Mech Eng 2007;196(21):2465-2477.
[18] Ghanem RG, Spanos PD. Stochastic finite elements: a spectral approach. Dover Pubns; 2003.
[19] Huang S, Quek S, Phoon K. Convergence study of the truncated Karhunen–Loeve expansion for simulation of stochastic processes. Int J Numer Methods Eng 2001;52(9):1029-1043.